



Density Functional Theory modeling and Monte Carlo simulation assessment of inhibition performance of two Quinoxaline Derivatives for Steel Corrosion

Y. Karzazi^{1,2,*}, M. E. Belghiti¹, F. El-Hajjaji³, S. Boudra⁴ and B. Hammouti¹

¹Laboratory of Applied Analytical Chemistry Materials and Environment,
Faculty of Sciences, University Mohammed Premier, P. O. Box 4808, 60046 Oujda, Morocco

²LSIA, National School of Applied Sciences, ENSA Al Hoceima,
University Mohammed Premier, P. O. Box 3, 32003 SidiBouafif, Morocco

³Laboratoire d'Ingénierie d'Electrochimie, Modélisation et d'Environnement (LIEME),
Faculty of Sciences, University Sidi Mohammed Ben Abdellah, Fez, Morocco

³Centre Régionale des Métiers de l'Éducation et de Formation, CRMEF, Tanger, Morocco

Received 13 July 2013, Revised 20 Sept 2014, Accepted 23 Sept 2014

*For correspondence: Email: karzazi@hotmail.com

Abstract

Quantum chemical calculations using the density functional theory (DFT) at the B3LYP/6-31G(d,p) level were performed on two quinoxaline derivatives named: 1-ethyl-3-methylquinoxalin-2(1H)-one (Et-N-Q=O) and 1-benzyl-3-methylquinoxalin-2(1H)-one (Bz-N-Q=O) in order to correlate the structural and electronic properties, such as HOMO, LUMO energy values, frontier orbital energy gap, molecular dipole moment (μ), electron affinity (A), ionization potential (I), electronegativity (χ), global hardness (η), softness (σ), the fraction of electron transferred (ΔN), electrophilicity index (ω), back-donation ($\Delta E_{\text{back-donation}}$) and Mulliken charges with the inhibitive action of these inhibitors on the mild steel corrosion in molar hydrochloric acid. Monte Carlo simulations were also executed to simulate the adsorption of the two quinoxaline derivatives on Fe (111) surface in the presence of molecules of water and the results show that Bz-N-Q=O is the most effective as corrosion inhibitor for mild steel in 1 M HCl medium.

Keywords: Corrosion; Inhibition; Mild steel; HCl medium; DFT; Electronic properties; Monte Carlo simulation.

1. Introduction

Mild steel is widely used in several industries as construction material due to its high mechanical properties and low-cost [1,2]. However, it is a highly reactive alloy and is very prone to corrosion during many industrial processes including acid cleaning, etching, acid pickling, and acid descaling [3,4]. Among the various available methods of corrosion protection, the consumption of the synthetic corrosion inhibitors is one of the most practical and cost effective method [5,6]. The use of acid solutions for these industrial activities results in loss corrosion and eventually loss of metals. Addition of organic corrosion inhibitors, which are compounds that contain heteroatoms (=N-, -O- and -S-), double and triple bonds, and aromatic rings, has been identified as one of the most practical and economical ways of controlling metal corrosion [7–10]. These compounds inhibit metallic corrosion by becoming adsorbate at metal/electrolyte interfaces in which polar functional groups such –NH₂, –OH, –C=N, =C-N-O ...etc. and pi-electrons of the double and triple bonds and aromatic rings act as adsorption centers [11]. Adsorption of these compounds depends upon several factors including molecular weight, nature of substituents, solution temperature, nature of inhibitor and electrolytes [12,13]. Nevertheless, most of the previously existing corrosion inhibitors are toxic and non-environmental friendly [14–16]. However, the use of

organic inhibitors in acid solutions can, in some cases, lead to enhancement of the metal corrosion [17], and stimulation of corrosion is correlated not only to the type and structure of the organic molecule but also depends on the type of acid and its concentration [18-21]. The corrosion inhibition, normally considered by corrosion scientists, is the relation between the molecular/electronic structures and corrosion inhibition efficiency.

In the last decades, plentiful researches were dedicated to give more explanation to the obtained efficiency of quinoxaline derivatives to numerous applications at several fields such as inhibition of corrosion for steel, Aluminum and copper in acidic medium [22-25], anti-viral [26], anti-bacterial [27], anti-inflammatory [28], anti-protozoal [29], anti-cancer [30,31] anti-depressant [32], anti-HIV [33], and as kinase inhibitors [34]. They are also used in the agricultural field as fungicides, herbicides, and insecticides [35].

In the present paper, molecular dynamics (MD) and quantum chemistry (DFT) are employed to discuss the relationship between inhibition efficiency and molecular structure of two quinoxaline derivatives (Figure 1) and to elucidate the mechanism of adsorption. To the best of our knowledge, connection between the structural parameters and corrosion inhibition of these compounds has not been reported in open literature.

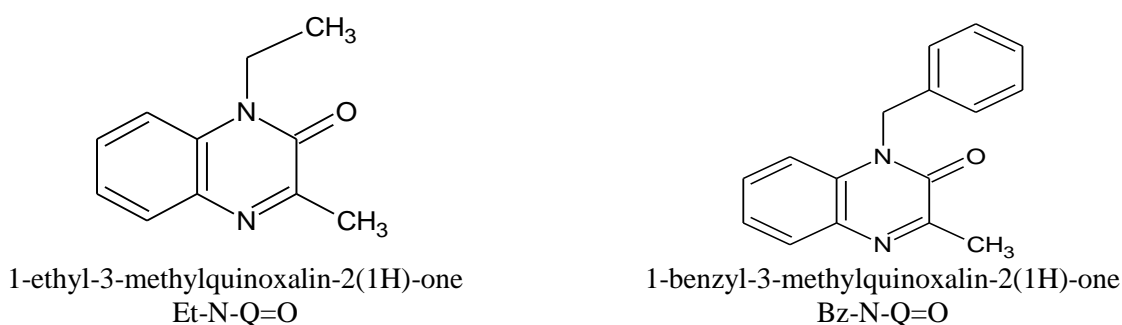


Figure 1. The chemical structures of investigated inhibitors Et-N-Q=O and Bz-N-Q=O.

2. Molecular simulations and quantum chemical calculations

2.1. Theory and computational details

Quantum chemical calculations have been proved to be a powerful tool for studying corrosion inhibition mechanism [36-38]. Density Functional theory (DFT), based on Beck's three parameter exchange functional and Lee-Yang-Parr nonlocal correlation functional (B3LYP) [39-41] and the 6-31G(d, p) orbital basis sets for all atoms as implemented in Gaussian 09 program [42], was performed on Pr-N-Q=O and Pr-N-Q=S in order to describe the interaction between the inhibitors molecules and the surface as well as the properties of these inhibitors concerning their reactivity. Hence, the geometries of molecules under study, in aqueous phase, were fully optimized with no constraints using DFT at the B3LYP/6-31G(d,p) level. All the calculations were performed in the presence of a solvent (water) by placing the solute in a cavity within the solvent reaction field. The Polarizable Continuum Model (PCM) using the integral equation formalism variant (IEFPCM) which is a self-consistent reaction field (SCRf) was used for water phase calculations [43]. Hereafter, we have investigated the relationship between the molecular, the electronic structure and the inhibition efficiency of the two studied molecules. For these seek, some molecular descriptors most relevant to their potential action as corrosion inhibitors, such as HOMO and LUMO energy values, frontier orbital energy gap, molecular dipole moment (μ), electron affinity (A), ionization potential (I), electronegativity (χ), global hardness (η), softness (σ), the fraction of electron transferred (ΔN), electrophilicity index (ω) and back-donation ($\Delta E_{\text{back-donation}}$), were calculated using the DFT method and have been used to understand the properties and activity of the newly prepared compounds and to help in the explanation of the experimental data obtained for the corrosion process.

The frontier orbital HOMO and LUMO of a chemical species are very important in defining its reactivity. A good correlation has been found between the speeds of corrosion and E_{HOMO} that is often associated with the electron donating ability of the molecule. Survey of literature shows that the adsorption of the inhibitor on the metal surface can occur on the basis of donor-acceptor interactions between the π -electrons of the heterocyclic compound and the vacant d-orbital of the metal surface atoms [44]., high value of E_{HOMO} of the molecules shows

its tendency to donate electrons to appropriate acceptor molecules with low energy empty molecular orbitals. Increasing values of E_{HOMO} facilitate adsorption and therefore enhance the inhibition efficiency, by influencing the transport process through the adsorbed layer. Similar relations were found between the rates of corrosion and ΔE ($\Delta E = E_{\text{LUMO}} - E_{\text{HOMO}}$) [43, 45-46]. The energy of the lowest unoccupied molecular orbital indicates the ability of the molecule to accept electrons. The lower the value of E_{LUMO} , the more probable the molecule would accept electrons. Consequently, concerning the value of the energy gap ΔE , larger values of the energy difference will provide low reactivity to a chemical species. Lower values of the ΔE will render good inhibition efficiency, because the energy required to remove an electron from the lowest occupied orbital will be low [47]. Another method to correlate inhibition efficiency with parameters of molecular structure is to calculate the fraction of electrons transferred from inhibitor to metal surface. According to Koopman's theorem [48], E_{HOMO} and E_{LUMO} of the inhibitor molecule are related to the ionization potential (I) and the electron affinity (A), respectively. The ionization potential and the electron affinity are defined as $I = -E_{\text{HOMO}}$ and $A = -E_{\text{LUMO}}$, respectively. Then absolute electronegativity (χ) and global hardness (η) of the inhibitor molecule are approximated as follows [47]:

$$\chi = \frac{I+A}{2}, \quad \chi = -\frac{1}{2}(E_{\text{HOMO}} + E_{\text{LUMO}})$$

$$\eta = \frac{I-A}{2}, \quad \eta = -\frac{1}{2}(E_{\text{HOMO}} - E_{\text{LUMO}})$$

As hardness (η), softness (S) is a global chemical descriptor measuring the molecular stability and reactivity and is given by:

$$S = \frac{1}{\eta}, \quad S = -2/(E_{\text{HOMO}} - E_{\text{LUMO}})$$

The chemical hardness fundamentally signifies the resistance towards the deformation or polarization of the electron cloud of the atoms, ions or molecules under small perturbation of chemical reaction. A hard molecule has a large energy gap and a soft molecule has a small energy gap [48]. The global electrophilicity index was introduced by Parr as a measure of energy lowering due to maximal electron flow between donor and acceptor and is given by [49]:

$$\omega = \left(\frac{\mu^2}{2}\right) S, \quad \omega = \frac{(I+A)}{8}$$

According to the definition, this index measures the propensity of chemical species to accept electrons. A good, more reactive, nucleophilic is characterized by lower value of μ , ω ; and conversely a good electrophilic is characterized by a high value of μ , ω . This new reactivity index measures the stabilization in energy when the system acquires an additional electronic charge ΔN from the environment. Thus the fraction of electrons transferred from the inhibitor to metallic surface, ΔN , is given by [50]:

$$\Delta N = \frac{\chi_{\text{Fe}} - \chi_{\text{inh}}}{2(\eta_{\text{Fe}} + \eta_{\text{inh}})}$$

Where χ_{Fe} and χ_{inh} denote the absolute electronegativity of iron and inhibitor molecule, respectively; η_{Fe} and η_{inh} denote the absolute hardness of iron and the inhibitor molecule, respectively.

In order to calculate the fraction of electrons transferred, a theoretical value of $\chi_{\text{Fe}} = +7.0$ eV [51] and $\eta_{\text{Fe}} = 0$ (eV)⁻¹ by assuming that for a metallic bulk $I = A$, because they are softer than the neutral metallic atoms [52]. According to the simple charge transfer model for donation and back donation of charges [53], when a molecule receives a certain amount of charge, ΔN^+ ; then:

$$\Delta E^+ = \mu + \Delta N^+ + \frac{1}{2}\eta (\Delta N^+)^2 \quad (a)$$

While when a molecule back-donates a certain amount of charge, ΔN^- , then:

$$\Delta E^- = \mu^- \Delta N^- + \frac{1}{2}\eta (\Delta N^-)^2 \quad (b)$$

If the total energy change is approximated by the sum of the contributions of Eqs. (a) and (b), assuming that the amount of charge back-donation is equal to the amount of charge received, $\Delta N^+ + \Delta N^- = 0$, then;

$$\Delta E_T = \Delta E_{\text{back-donation}} = \Delta E^+ + \Delta E^- = (\mu^+ + \mu^-) \Delta N^+ + \frac{1}{2}\eta (\Delta N^+)^2 + \frac{1}{2}\eta (\Delta N^-)^2$$

$$\Delta E_{\text{back-donation}} = (\mu^+ + \mu^-) \Delta N^+ + \eta (\Delta N^+)^2; \quad (\Delta N^+ = -\Delta N^-)$$

The most favorable situation corresponds to the case when the total energy change ($\Delta E_{\text{back-donation}}$) becomes a minimum with respect to ΔN^+ , which implies that $(\Delta N^+ = -(\mu^+ + \mu^-) / 2\eta)$ and that;

$$\Delta E_{\text{back-donation}} = -(\mu^+ - \mu^-)^2 / 4\eta = -\frac{\eta}{4} \quad \Delta E_{\text{back-donation}} = \frac{1}{8}(E_{\text{HOMO}} - E_{\text{LUMO}})$$

The $\Delta E_{\text{back-donation}}$ implies that when $\eta > 0$ and $\Delta E_{\text{back-donation}} < 0$ the charge transfer to a molecule, followed by a back-donation from the molecule, is energetically favoured. In this context, hence, it is possible to compare the stabilization among inhibiting molecules, since there will be an interaction with the same metal, then, it is expected that it will decrease as the hardness increases.

2.2. Monte Carlo simulations

The Monte Carlo (MC) search was used to calculate the low configuration adsorption energy of the interactions of two quinoxaline derivatives on clean iron surface. Metropolis Monte Carlo (MC) simulations methodology [54] using the DMol-3 code [55-56] and Adsorption Locator [57-58] implemented in the BOVIA Material Studio 8.0 (Accelrys, San Diego, CA, USA) [59], has been used to build the system adsorbate/substrate. Simulations were carried out with a slab thickness of 5Å, a super cell of (6 × 6) and a vacuum of 30 Å along the C-axis in a simulation box (25.17Å x 25.37Å x 40.26Å) with periodic boundary conditions to model a representative part of the interface devoid of any arbitrary boundary effects. For the whole simulation procedure, the COMPASS force field (condensed-phase optimized molecular potentials for atomistic simulation studies) [60] was used to optimize the structures of all components of the corrosion system (metal substrate / inhibitor / solvent molecules). To mimic the real corrosion environment, 30 molecules of water were added to the simulation box. This computational study aims to find low-energy adsorption sites to investigate the preferential adsorption of inhibitor molecules on iron surface aiming to find a relationship between the effect of its molecular structure and its inhibition efficiency.

3. Results and discussion

3.1. Calculations of the quantum chemical descriptors

The inhibition of mild steel using two quinoxaline derivatives; Bz-N-Q=O and Et-N-Q=O as corrosion inhibitors were explored experimentally, the classification of these inhibitors according to their corrosion inhibition efficiency is: Bz-N-Q=O > Et-N-Q=O (48 % > 44 %, respectively) [61]. The inhibitive performance of Bz-N-Q=O advocates a quite strong bonding of this quinoxaline molecules onto the metal surface due to the existence of several lone pairs from heteroatoms and π -orbitals, blocking the active sites and hence reducing the corrosion rate. Accordingly, quantum chemical calculations based on DFT method, at the B3LYP/6-31G(d,p) level, were performed to investigate the effect of structural parameters on the inhibition efficiency of inhibitors and study their adsorption mechanisms on the metal surface. The geometric and electronic structures of Bz-N-Q=O and Et-N-Q=O in solvent phase (water) were calculated from optimized structures and are presented in Fig. 2.

In this work, the optimized geometries with the DFT at the B3LYP/6-31G(d,p) level of the two inhibitors are essentially planar. This may facilitate the donation of π -electrons by the aromatic rings, the nonbinding electron pair of nitrogen in quinoxaline molecules as well as the oxo group. The ground state geometry of the inhibitor as well as the nature of its frontier molecular orbitals, explicitly, the highest occupied molecular orbital (HOMO) and the lowest unoccupied molecular orbital (LUMO) are involved in the activity properties of the inhibitors.

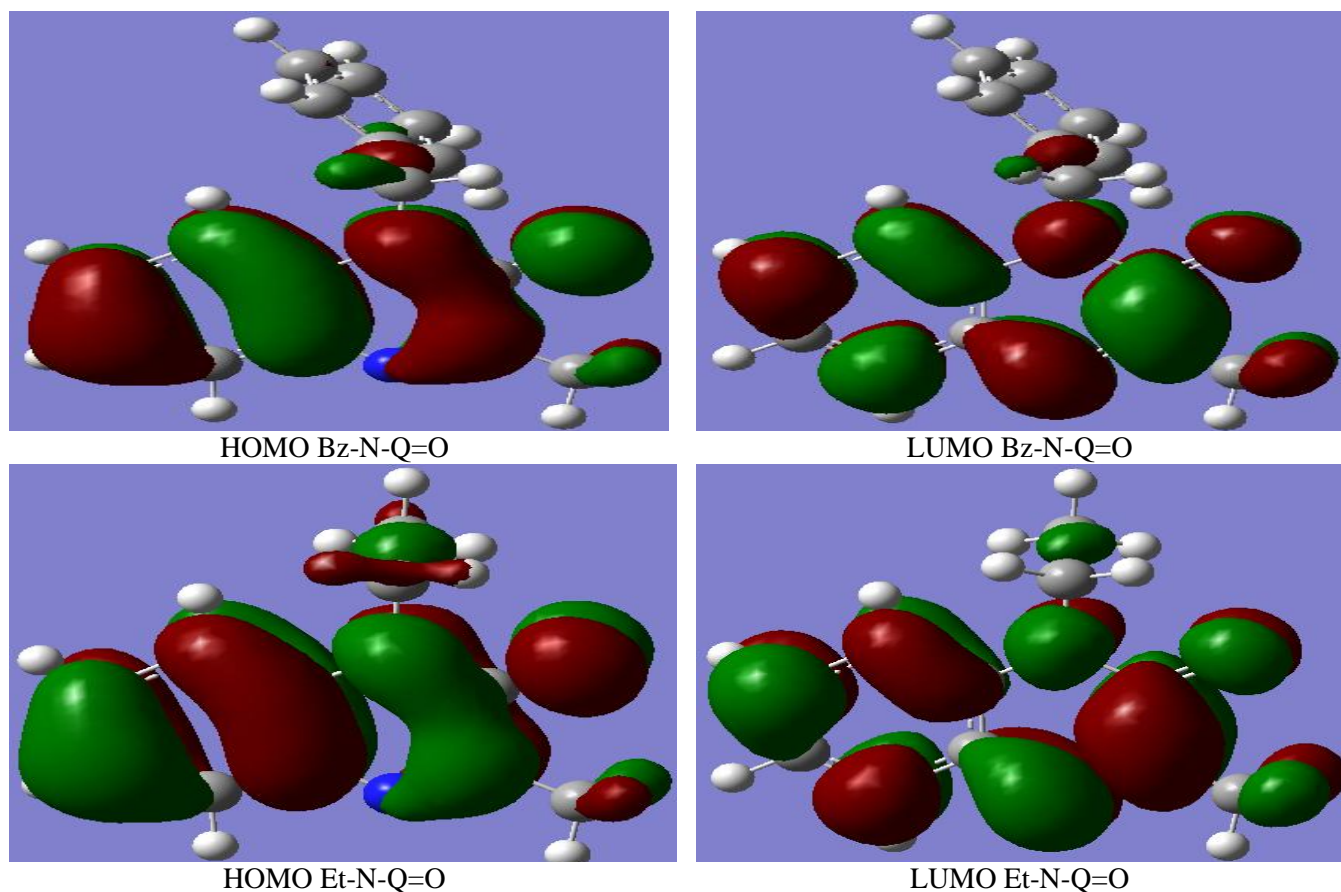


Figure 3. Schematic representations of HOMO and LUMO molecular orbitals of studied molecules of Bz-N-Q=O and Et-N-Q=O calculated in solvent phase (water) with the DFT at the B3LYP/6-31G(d,p) level.

Energy band Gap (ΔE_{gap}) is an essential parameter, which provides a measure for the stability of the inhibitor molecule towards the adsorption on metallic surface (physisorption & chemisorption). In this work, Bz-N-Q=O showed good inhibitory effect against the corrosion of iron in hydrochloric acid solution and is considered to be the most effective. The results obtained in Table 4 demonstrate that the compound Et-N-Q=O has the lowest ΔE_{gap} (+4.3764 eV); this means that the molecule could have better performance as corrosion inhibitor. The trend of the calculated values of the Energy band Gap (ΔE_{gap}) for Bz-N-Q=O and Et-N-Q=O did not correlate significantly with the trend of experimental inhibition efficiency values. This is due to the type of adsorption mechanism of the Pr-N-Q=O and Bz-N-Q=O on mild steel surface in 1 M HCl solution. However, physical adsorption seems to be more probable and predominantly favorable than chemisorption.

Ionization energy ($IE = -E_{\text{HOMO}}$) is an important descriptor of the chemical reactivity of atoms and molecules. High ionization energy designates high stability and chemical inertness and small ionization energy specifies high reactivity of the atoms and molecules [64]. The high ionization energy ($IE = 6.1473\text{eV}$) of Et-N-Q=O indicates the high inhibition efficiency. The trend of the calculated values of the Ionization energy for Bz-N-Q=O and Et-N-Q=O correlate significantly with the trend of experimental inhibition efficiency values.

Dipole moment, μ (Debye), is another important electronic parameter that results from non-uniform distribution of charges on the various atoms in the molecule [65]. The high value of μ (Debye) probably increases the adsorption between the chemical compound and the metal surface [66]. The energy of the deformability increases with the increase in μ , making the molecule easier to adsorb at the iron (Fe) surface. The volume of the inhibitor molecules ($\text{Bz-N-Q=O} > \text{Et-N-Q=O}$) also increases with the increase of μ . This increases the contact area between the molecule and the surface of iron and increases the corrosion inhibition ability of inhibitors. In

our study, there is no direct relationship between the inhibition efficiency and the dipole moment (probably the molecule Bz-N-Q=O may be adsorbed on the metal surface by horizontal or vertical form, involving the displacement of water molecules from the mild steel surface).

Table 4. Quantum chemical parameters for the molecules Bz-N-Q=O and Et-N-Q=O obtained in solvent phase (water) with the DFT at the B3LYP/6-31G(d, p) level.

Quantum Chemical Parameters	Bz-N-Q=O	Et-N-Q=O
E_{LUMO} (eV)	-1.8340	-1.7709
E_{HOMO} (eV)	-6.2135	-6.1473
ΔE (eV)	+4.3794	4.3764
IP (eV)	6.2135	6.1473
EA (eV)	1.8340	1.7709
χ (eV)	4.0237	3.9591
η (eV)	2.1897	2.1882
μ (debye)	4.2304	4.3427
ω (eV)	4.0865	4.3093
S (eV) ⁻¹	0.4567	0.4570
ΔN	0.6796	0.6948
$\Delta E_{back-donation}$ (eV) ⁻¹	-0.5474	-0.5471
Total energy (a.u)	-802.9198	-611.1804

The absolute electronegativity (χ) is the chemical property that describes the ability of a molecule to attract electrons towards itself in a covalent bond. According to Sanderson's electronegativity equalization principle [67], the molecule Bz-N-Q=O with a high electronegativity quickly reaches equalization and hence low reactivity is expected which in turn indicates low inhibition efficiency. The Table 4 shows that the highest electronegativity is encountered for Bz-N-Q=O. Hence an increase in the difference of electronegativity between the metal and inhibitor is observed at the largest extent for Bz-N-Q=O. This is in good agreement with the experimental results.

Mulliken population analysis is carried out to determine the electron rich groups/atoms for the molecules under study and is therefore used to evaluate the adsorption centers of inhibitors since this method has been generally reported and it is commonly used for the calculation of the charge distribution over the entire skeleton of the molecule [68]. There is a general unanimity by many authors that the more negatively charged heteroatom is, the more is its ability to absorb on the metal surface through a donor-acceptor type reaction [69]. Variation in the inhibition efficiency of the two inhibitors under study depends on the presence of electronegative Oxygen and Nitrogen atoms in their molecular structure. The site of ionic reactivity could be estimated from the net charges on a molecule. Table 5 representing the effective atomic charges Mulliken populations of Bz-N-Q=O and Et-N-Q=O inhibitors in aqueous solution, shows that oxygen and nitrogen (=N-, -O-) atoms and some carbon atoms carry more negative charges, while the remaining carbon atoms carry more positive charges. This means that the atoms carrying negative charges are the negative charge centers, which can offer electrons to the Fe atoms to form coordinate bond, and the atoms carrying positive charges are the positive charge centers, which can accept electrons from orbital of Fe atoms to form feedback bond. The calculated Mulliken charges at the B3LYP/6-31G(d, p) level for the Bz-N-Q=O and Et-N-Q=O inhibitors are in good agreement with the delocalization of charges, discussed in Table 5, leading to an excess of negative charges on the nitrogen(=N-) and oxygen(-O-) atoms of the quinoxaline ring. We emphasize also that the highest negative charges were found for the atoms C1, C2, C5, C6, N13, O14, C15, C18, N22, C24, C26, C28 and C30 while the highest positive charges were found for the atoms C3, C4, C11 and C23 for the Bz-N-Q=O. These findings are attributed to the electronegativity of the oxygen and nitrogen atoms. Besides, the atoms (C15, C16, C17, C 19, C20 and C35) bear significant negative

charges. Thus, the optimized structure is in accordance with the fact that excellent corrosion inhibitors cannot only offer electrons to unoccupied orbital of the metal, but also accept free electrons from the metal. Therefore, it can be inferred that Quinoxaline ring ($=C-N=$, $=N-C=O$), the anisyl substituent (methyl-phenyl) for Bz-N-Q=O (respectively the Ethyl for Et-N-Q=O) are the possible active adsorption sites. Noteworthy, the heteroatoms in Bz-N-Q=O are more negatively charged than Et-N-Q=O. These results corroborate the experimental results, where among the two quinoxaline derivatives under study, Bz-N-Q=O is the best inhibitor.

Table 5. Calculated Mulliken atomic charges for heavy atoms of Bz-N-Q=O and Et-N-Q=O in solvent phase using DFT at the B3LYP/6-31G (d,p) basis set.

Bz-N-Q=O		Et-N-Q=O	
C1	-0.1039	C1	-0.1051
C2	-0.1138	C2	-0.1138
C3	+0.2187	C3	+0.2181
C4	+0.3567	C4	+0.3563
C5	-0.1231	C5	-0.1335
C6	-0.1072	C6	-0.1068
C11	+0.5983	C11	+0.5876
C12	+0.2363	C12	+0.2370
N13	-0.5790	N13	-0.5764
O14	-0.5793	O14	-0.5769
C15	-0.1442	C15	-0.0749
C18	-0.3615	C18	-0.3228
N22	-0.5385	C22	-0.3616
C23	+0.1134	N26	-0.5401
C24	-0.1369		
C25	-0.1241		
C26	-0.0998		
C28	-0.1000		
C30	-0.0993		

From the theoretical calculations carried on the inhibitors molecular systems in solvent phase (water) with the DFT at B3LYP/6-31G (d,p) level, good correlation coefficients of the inhibition efficiencies with electronic properties was obtained. Therefore, theoretical calculations on these molecules could be a good approach for the study of their potential inhibition capability of metal corrosion in hydrochloric acid.

3.2. Monte Carlo simulations Bz-N-Q=O and Et-N-Q=O

In the current study, the MC simulation was performed to study the behavior of the system (single inhibitor molecule / iron surface) in water as solvent. The single molecules of (Bz-N-Q=O and Et-N-Q=O) on Fe (111) surface configuration are sampled from a canonical ensemble. The total energy, Van der Waals energy, average total energy, electrostatic energy and intermolecular energy for the systems under study; Fe (111) / (Bz-N-Q=O and Et-N-Q=O) in water as solvent are calculated by optimizing the whole system and given in Figure 4.

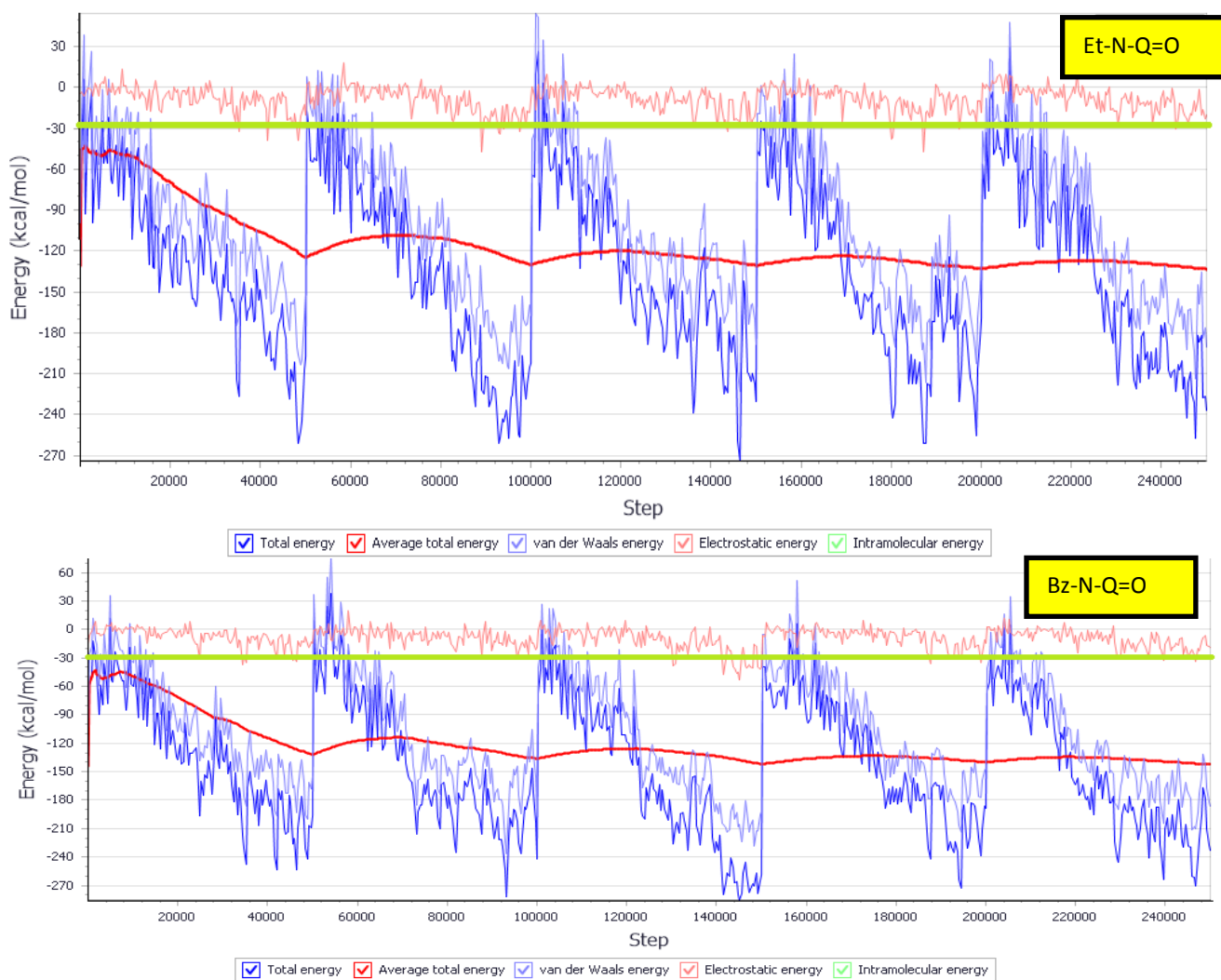


Figure 4. Total energy distribution for Fe (111) / (Et-N-Q=O or Bz-N-Q=O) / 30 H₂O complexes during energy optimization process.

The most stable low energy adsorption configurations of the inhibitors (Et-N-Q=O and Bz-N-Q=O) adsorbed onto the iron (111) surface in water solvent molecules (30 H₂O) using MCs are depicted in Figure 5. Side and top views of stable adsorption configurations for the inhibitors under study on Fe(111) / 30 H₂O system using Monte Carlo simulations are given in Figure 5.

From Figure 5 we show that the adsorption centers of the both inhibitors on the iron (111) surface in water solvent molecules are the π -electrons of quinoxaline ring, nitrogen (-N=) and oxygen (-O-) heteroatoms. For the Et-N-Q=O and Bz-N-Q=O inhibitor molecules, the calculated dihedral angles around the quinoxaline ring are close to 0° or 180°, demonstrating planarity of the quinoxaline ring. Thus, the Et-N-Q=O and Bz-N-Q=O inhibitor molecules adsorbed nearly plane (on the level of the quinoxaline ring) on the iron (111) surface in water solvent molecules to maximize surface coverage and contact than Et-N-Q=O and Bz-N-Q=O inhibitors (Figure 5), guaranteeing the interaction between adsorbate and substrate. This finding is in good agreement with our experimental results.

The values for the outputs and descriptors calculated by the Monte Carlo simulations for Fe (111) / (Et-N-Q=O or Bz-N-Q=O) / 30 H₂O systems are listed in Table 6. The parameters presented in Table 6 include total energy (E_{Total}), in Kcal/mol, of the substrate-adsorbate configuration. The total energy is defined as the sum of

the energies of the adsorbate components. The total energy of the inhibitors on iron surface in the presence of water follows the trend, Bz-N-Q=O < Et-N-Q=O. Hence, the inhibitor Bz-N-Q=O is the most stable between the two inhibitors.

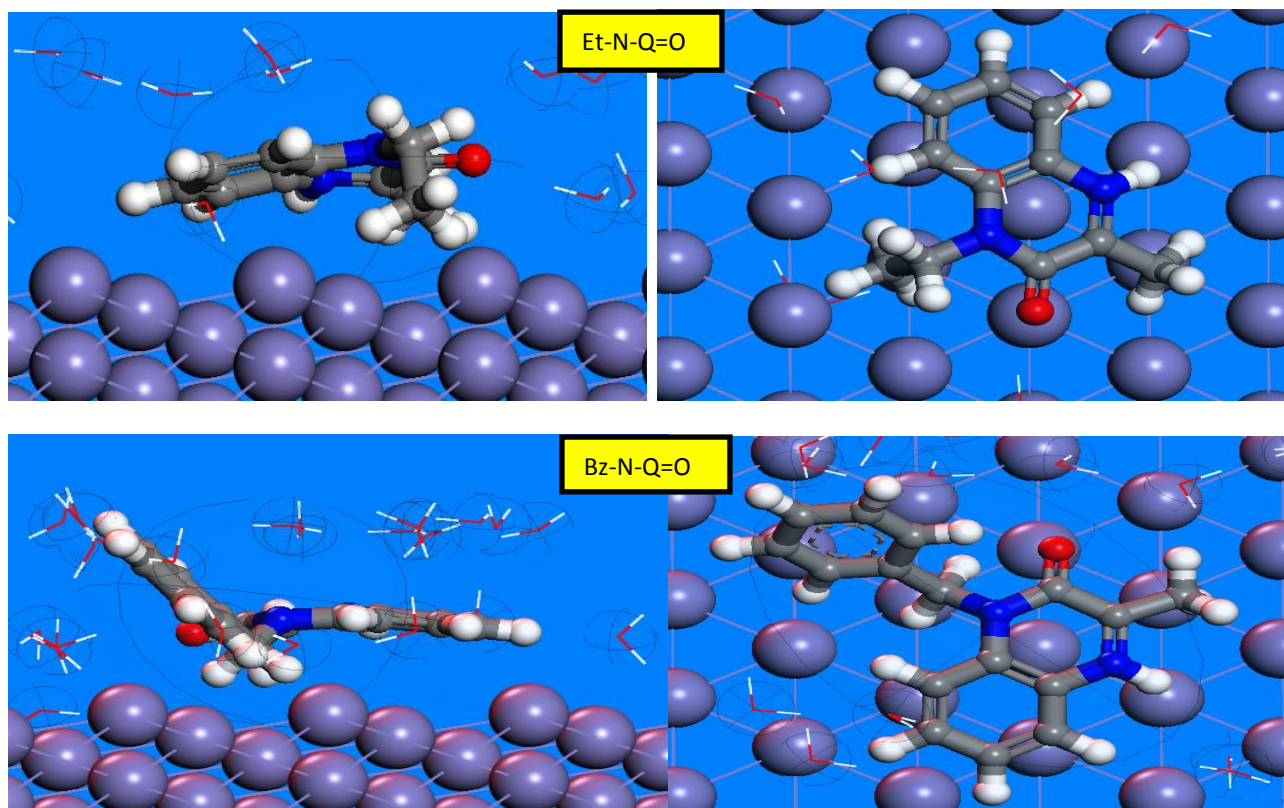


Figure 5. Side and top views of stable adsorption configurations for Fe (111) / (Et-N-Q=O or Bz-N-Q=O) / 30 H₂O complexes obtained using the Monte Carlo simulations.

Table 6. Outputs and descriptors for the lowest adsorption configurations for Fe (111) / (Et-N-Q=O, or Bz-N-Q=O) / 30 H₂O systems calculated by Monte Carlo simulation. (All values are given in Kcal/mol).

Inhibitors	E_{Total}	E_{Ads}	R.A.E	D_{Energy}	$\frac{dE_{ads}}{dN_i}$ Inhs	$\frac{dE_{ads}}{dN_i}$ Water
Et-N-Q=O	-412.90	-386.06	-385.47	-0.59	-101.42	-0.57
Bz-N-Q=O	-425.80	-404.93	-409.22	4.29	-104.40	-0.61

The adsorption energy (E_{Ads}), in Kcal/mol, reports energy released (or required) when the relaxed adsorbate components (Et-N-Q=O and Bz-N-Q=O) are adsorbed onto the substrate (Fe (111) surface). It is generally accepted that the main mechanism of corrosion inhibitor interaction with steel is by adsorption. Therefore, the adsorption energy may help us to rank inhibitor molecules [70-71]. From Table 6, it is quite clear that the adsorption energies values are negative, which denote that the adsorption could occur spontaneously [72].

The adsorption energy of the inhibitor molecules Bz-N-Q=O and Et-N-Q=O is -425.80 Kcal/mol and -412.90 Kcal/mol, respectively, which means that adsorption of Bz-N-Q=O molecule on iron (111) surface in water solvent molecules is slightly high than that of Et-N-Q=O. This is due to the presence of donor group (methyl-phenyl) attached to quinoxaline ring on the structure, which serves as additional active centres. The adsorption energies of the inhibitors on iron surface in the presence of water decreased in the order: Bz-N-Q=O > Et-N-Q=O. This ordering shows that the system with the most stable and stronger adsorption is Fe (111) / Bz-N-Q=O. Hence, Bz-N-Q=O is the best corrosion inhibitor between the two inhibitors under study. Besides, the relatively small

negative values for the adsorption energy of the inhibitor molecules Bz-N-Q=O than Et-N-Q=O suggest that the adsorption mechanism of the Bz-N-Q=O and Et-N-Q=O inhibitors, on mild steel surface in 1 M HCl solution as typical of physisorption[73]. Therefore our Monte Carlo results are in good agreement with the experiment where the inhibition efficiency (IE) for inhibitor Bz-N-Q=O is slightly higher than Et-N-Q=O. The observed trend experimentally (Bz-N-Q=O > Et-N-Q=O) is consistent with our Monte Carlo results.

In this work, the substrate energy is taken as zero. The adsorption energy is defined as the sum of the rigid adsorption energy (R.A.E) and the deformation energy for the adsorbate components. The rigid adsorption energy reports the energy, in Kcal/mol, released (or required) when the unrelaxed molecules, (Et-N-Q=O & Bz-N-Q=O,) before the geometry optimization step are adsorbed on the iron (111) surface in presence of 30 molecules of water. The deformation energy (D_{Energy}) reports the energy, in Kcal/mol, released when the adsorbed component molecule (Et-N-Q=O & Bz-N-Q=O) is relaxed on the iron surface. Table 6 shows also (dE_{ads}/dN_i), which reports the energy, in Kcal/mol, of Fe-components configurations (Et-N-Q=O and Bz-N-Q=O) where one of the inhibitor molecules has been removed.

Conclusions

Density Functional Theory at the B3LYP level and Monte Carlo simulation were employed to evaluate the corrosion inhibition activity of two quinoxaline derivatives at the molecular level. The inhibition efficiencies of these compounds seem to be determined by the conjugation of electronic factors and molecular geometry. The analysis of the HOMO, LUMO, and partial atomic charges suggests the centers that would be preferred for nucleophilic or electrophilic attack. The theoretical calculations at the B3LYP level carried on the inhibitors molecular systems in solvent phase (water) show good correlation of the inhibition efficiencies with the electronic properties of the inhibitors under study. In fact, the trend followed by most of the quantum parameters is in conformity with that of the experimental inhibition efficiency (Bz-N-Q=O > Et-N-Q=O). Therefore, theoretical calculations on these molecules could be a good approach for the study of their potential inhibition capability of metal corrosion in hydrochloric acid. Monte Carlo simulations were further performed to simulate the adsorption of the two quinoxaline derivatives on Fe (111) surface in the presence of molecules of water and the results show that Bz-N-Q=O is the most effective as corrosion inhibitor for mild steel in 1 M HCl medium. We have established using Monte Carlo simulations that the order of adsorption of the inhibitors under study on iron surface agrees with the experimental trend. The inhibitor Bz-N-Q=O has the strongest interaction with the steel surface than the other inhibitor, which corroborate very well with our experimental results.

Acknowledgments-Y.K. appreciates the Laboratory for Chemistry of Novel Materials, University of Mons, Belgium, for the access to the computational facility.

References

1. Sasikumar Y., Adekunle AS., Olasunkanmi LO., Bahadur I., Baskar R., Kabanda MM., Obot IB., Ebenso EE., *J. Mol. Liq.*, 211 (2015) 105–118.
2. Verma C., Quraishi MA., Olasunkanmi LO., Ebenso EE., *RSC Adv.*, 5 (2016)85417–85430.
3. Yadav M., Kumar S., Tiwari N., Bahadur I., Ebenso EE., *J. Mol. Liq.*, 212 (2015)151–167.
4. Yadav M., Kumar S., Sinha RR., Bahadur I., Ebenso EE., *J. Mol. Liq.*, 211 (2015)135–145.
5. Verma C., Singh A., Quraishi MA., *J. Mol. Liq.*, 212 (2015) 804–812.
6. Yadav M., Kumar S., Bahadur I., Ramjugernath D., *Int. J. Electrochem. Sci.*, 9 (2014)6529–6550.
7. Belghiti ME., Tighadouini S., Karzazi Y., Dafali A., Hammouti B., Radi S., Solmaz R., *J. Mater. Environ. Sci.*, 7 (1) 337-346, 2016.
8. Belghiti ME., Karzazi Y., Tighadouini S., Dafali A., Jama C., Warad I., Hammouti B., Radi S., *J. Mater. Environ. Sci.*, 7 (3) 956-967, 2016.
9. Murulana LC., Kabanda MM., Ebenso EE., *RSC Adv.*, 5 (2015) 28743–28761.
10. Verma C., Quraishi MA., Singh A., *J. Mol. Liq.*, 212 (2015) 804–812.
11. Verma C., Ebenso EE., Bahadur I., Obot IB., Quraishi MA., *J. Mol. Liq.*, 212 (2015) 209–218.

12. Barbosa da Silva A., D'Elia E., Gomes JACP., *Corros. Sci.*, 52 (2010) 788–793.
13. Verma C., Quraishi MA., Singh A., Taibah J., *Uni. Sci.* (2016), <http://dx.doi.org/10.1016/j.jtusci.2015.10.005>.
14. Kardas G., Solmaz R., *Corros. Rev.*, 24, (3), 151–172.
15. Verma C., Olasunkanmi LO., Obot IB., Ebenso EE., Quraishi MA., *RSC Adv.*, 6 (2016)15639–15654.
16. Bousskri A., Anejjar A., Messali M., Salghi R., Benali O., Karzazi Y., Jodeh S., Zougagh M., Ebenso E.E., Hammouti B., *J. Mol. Liq.*, 211, 1000-1008, 2015.
17. Lagrenee M., Mernari B., Chaibi N., Traisnel M., Vezin H and Bentiss F., *Corros. Sci.*, 43 (2001) 951.
18. Chetouani A. & Hammouti B., *Molecular modelling Quantum Chemical Studies and Corrosion Inhibitors - Synthesis and Use of New Heterocyclic and polymers for the Protection of Steel in Acid Medium*, ISBN: 978-3-659-39805-6, Lambert Academic Publishing., (2013) 1-167.
19. Aouniti A., Khaled KF. Hammouti B., *Int. J. Electrochem. Sci.*, 8 (2013) 5925-5943.
20. Krim O., Elidrissi A., Hammouti B., Ouslim A., Benkaddour M., *Chem. Eng. Comm.*, 196 (12) (2009) 1536-1546.
21. Sulaiman KO., A. T. Onawole *Computational and Theoretical Chemistry*.1093 (2016) 73-80.
22. Zarrouk A., El Ouali I., Bouachrine M., Hammouti B., Ramli Y., Essassi E. M., Warad I., Aouniti A., Salghi R., *Res. Chem. Intermed.*, 38 (2013) 1125-1133.
23. Zarrok H., Zarrouk A., Salghi R., Elmahi B., Hammouti B., Al-Deyab S.S., Ebn Touhami M., Bouachrine M., Oudda H., Boukhris S., *Int. J. Electrochem. Sci.*, 8 (2013) 11474-11491.
24. Zarrouk A., Bouachrine M., Hammouti B., Dafali A., Zarrok H., *J. Saudi Chem. Soc.*, 18 (5) (2014) 550-555.
25. Zarrouk A., Zarrok H., Ramli Y., Bouachrine M., Hammouti B., Sahibed-dine A., Bentiss F., *Journal of Molecular Liquids.*, 222 (2016) 239-252.
26. Loriga M., Piras S., Sanna P., Paglietti G., *Farmaco.*, 52 (1997) 157.
27. Seitz LE., SulingWJ., Reynolds RC., *J. Med. Chem.*, 45 (2002) 5604.
28. Yb K., Yh K., Jy P., SK K., *Bioorg. Med. Chem. Lett.*, 14 (2004) 541.
29. Hui X., Desrivot J., Bories C., Loiseau PM., Franck X., Hocquemiller R., Figadere B., *Bioorg. Med. Chem. Lett.*, 16 (2006) 815.
30. Lindsley CW., Zhao Z., Leister WH., Robinson RG., Barnett SF., Defeo-Jones D., Jones R.E., Hartman GD., Huff JR., Huber HE., Duggan ME., *Bioorg. Med. Chem. Lett.*, 15 (2005) 761.
31. Labarbera D. V., Skibo E.B., *Bioorg. Med. Chem.*, 13 (2005) 387.
32. Sarges R., Howard HR., Browne RG., Lebel LA., Seymour PA., Koe BK., *J. Med. Chem.*, 33 (1990) 2240.
33. Srinivas C., Kumar CNSSP., Rao VJ., Palaniappan S., *Journal of Molecular Catalysis A: Chemical* 265 (1) (2007) 227-230.
34. Ghoms NT., Ahabchane NEH., Es-Safi NE., Garrigues B., Essassi El M., *Spectroscopy Lett.*, 40 (2007) 741.
35. Sakata G., Makino K., Karasawa Y., *Heterocycles* 27 (1988) 2481.
36. Karzazi Y., Belghiti M.E., Dafali A., Hammouti B., *J. Chem. Pharm. Res.*, 6 (2014) 689-696.
37. Khadraoui A., Khelifa A., Boutoumi H., Mettai B., Karzazi Y., Hammouti B., *Portugaliae Electrochim. Acta* 32 (4) (2014) 271-280.
38. Belghiti ME., Dahmani M., Messali M., Karzazi Y., Et-Touhami A., Yahyi A., Dafali A., Hammouti B., *Der Pharma Chemica.*, 7 (5) (2015) 106-115.
39. Becke AD., *J. Chem. Phys.*, 96 (1992) 9489-9497.
40. Becke AD., *J. Chem. Phys.*, 98 (1993) 1372-1377.
41. Lee C., Yang W., Parr RG., *Phys. Rev.*, B 37 (1988) 785-789.
42. Frisch MJ., Trucks GW., Schlegel HB., Scuseria GE., Robb MA., Cheeseman JR., Scalmani G., Barone V., Mennucci B., Petersson GA., Nakatsuji H., Caricato M., Li X., Hratchian H. P., Izmaylov, J. Bloino AF., Zheng G., Sonnenberg JL., Hada M., Ehara M., Toyota K., Fukuda R., Hasegawa J., Ishida M., Nakajima T., Honda Y., Kitao O., Nakai H., Vreven T., Montgomery J. A., Jr., Peralta J. E., Ogliaro F., Bearpark M., Heyd JJ., Brothers E., Kudin KN., Staroverov VN., Kobayashi R., Normand J., Raghavachari K., Rendell A., Burant JC., Iyengar SS., Tomasi J., Cossi M., Rega N., Millam JM., Klene M., Knox JE., Cross JB., Bakken V., Adamo C., Jaramillo J., Gomperts R., Stratmann RE., Yazyev O., Austin AJ., Cammi R., Pomelli C., Ochterski JW., Martin RL., Morokuma K., Zakrzewski VG., Voth GA., Salvador P., Dannenberg JJ.,

- Dapprich S., Daniels AD., Farkas Ö., Foresman JB., Ortiz JV., Cioslowski J., Fox DJ., Gaussian, Inc. Wallingford CT, (2009).
43. Tomasi J., Mennucci B., Cammi R., *Chem. Rev.*, 105 (2005) 2999-3093.
 44. Domenicano A., Hargittai I., *Accurate Molecular Structures, Their Determination and Importance*, Oxford University Press, New York, 1992.
 45. Li W., Zhao X., Liu F., Deng J., Hou B., *Mater. Corros.* 60 (2009) 287-293.
 46. Saha SKr., Ghosh P., Chowdhury AR., Samanta P., Murmu NC., Lohar AKr., Banerjee P., *Can. Chem. Trans.* 2 (2014) 381-402.
 47. Wang H., Wang X., Wang H., Wang L., Liu A., *J. Mol. Model.*, 13 (2007) 147-153.
 48. Fleming I., *Frontier Orbitals and Organic Chemical Reactions*, John Wiley and Sons, New York, 1976.
 49. Parr RG., Szentpaly L., Liu S., *J. Am. Chem. Soc.*, 121 (1999) 1922-1924.
 50. Sastri VS., Perumareddi JR., *Corros. Sci.*, 53 (1997) 617-622.
 51. Morad MS., *Corros. Sci.*, 50 (2008) 436-448.
 52. Deward MJS. Thiel W., *J. Am. Chem. Soc.*, 99 (1977) 4899-4907.
 53. Gomez B., Likhanova NV., Dominguez-Aguilar MA., Vela R., Martinez-Palou A., Gasquez J., *J. Phys. Chem. B* 110 (2006) 8928-8934.
 54. Metropolis N., Rosenbluth AW., Rosenbluth MN., Teller AH., Teller E., *J. Chem. Phys.*, 21 (1953) 1087.
 55. Delley B., *J. Chem. Phys.*, 92 (1990) 508.
 56. Delley B., *J. Chem. Phys.*, 113 (2000) 7756.
 57. Frenkel D., Smit B., *Understanding Molecular Simulation: From Algorithms to Applications*, 2nd Edition, Academic Press, San Diego (2002).
 58. Kirkpatrick S., Gelatt CD., Vecchi MP., *Science.*, 220 (4598) (1983) 671-680.
 59. BIOVIA Materials Studio version 8.0, Accelrys Inc. USA., 2014.
 60. Karzazi Y., Belghiti M. E., El-Hajjaji F., Hammouti B., *J. Mater. Environ. Sci.* 7 (10) (2016) 3916-3929.
 61. El-Hajjaji F., Zerga B., Sfaira M., Taleb M., Ebn Touhami M., Hammouti B., Al-Deyab S.S., Benzeid H., Essassi El M., *J. Mater. Environ. Sci.*, 5 (1) (2014) 255-262.
 62. Musa AY., Kadhum AH., Mohamad AB., Rohoma AB., Mesmari H., *J. Mol. Struct.* 969(2010) 233-237.
 63. Gece G., Bilgic S., *Corros. Sci.* 51 (2009) 1876-1878.
 64. Sandip KR., Nazmul I., Dulal CG., *J. Quant. Infor. Sci.*, 1 (2011) 87-95.
 65. Kikuchi O., *Quant. Struct.-Act. Relat.* 6, 179 (1987).
 66. Li X., Deng S., Fu H., Li T., *Electrochim. Acta.* 54(2009)4089.
 67. Lukovits I., Kalman E., Zucchi F., *Corrosion.* 57 (2001) 3-8.
 68. Saha SKr., Ghosh P., Hens A., Murmu NC., Banerjee P., *Phys. E.* 66 (2015) 332-341.
 69. Saha SKr., Dutta A., Ghosh P., Sukul D., Banerjee P., *Phys. Chem. Chem. Phys.*, 17(2015) 5679-5790
 70. Belghiti ME., Karzazi Y., Dafali A., Hammouti B., Bentiss F., Obot IB., Bahadur I., Ebenso EE., *J. Mol. Liq.*, 218 (2016) 281-293.
 71. Belghiti ME., Karzazi Y., Dafali A., Obot I.B., Ebenso EE., Emrane KM., Bahadur I., Hammouti B., Bentiss F., *J. Mol. Liq.*, 216 (2016) 874-886.
 72. Ebenso EE., Kabanda MM., Arslan T., Saracoglu M., Kandemirli F., Urulana LC., Singh AK., Shukla SK., Hammouti B., Khaled KF., Quraishi MA., Obot IB., Eddy NO., *Int. J. Electrochem. Sci.*, 7 (2012) 5643-5676.

(2016) ; <http://www.jmaterenvirosci.com/>